Direct activation of genes involved in intracellular iron use by the yeast iron-responsive transcription factor Aft2 without its paralog Aft1.

Maïte Courel, Sylvie Lallet, Jean-Michel Camadro, Pierre-Louis Blaiseau

Direct activation of genes involved in intracellular iron use by the yeast iron-responsive transcription factor Aft2 without its paralog Aft1

Maïté COUREL, Sylvie LALLET, Jean-Michel CAMADRO, and Pierre-Louis BLAISEAU*

Laboratoire d'Ingénierie des Protéines et Contrôle Métabolique

Département de Biologie des Génomes, INSTITUT JACQUES-MONOD

UMR 7592 CNRS - Universités Paris 6 & 7

2 Place Jussieu , F-75251 Paris cedex 05 France

* Corresponding author: E-mail: blaiseau@ijm.jussieu.fr

Tel: (33) 1 44 27 47 41

Fax: (33) 1 44 27 57 16

Running title: Transcriptional regulation of iron metabolism in yeast

Word count: Materials and Methods: 1157

Introduction, Results and Discussion: 4724

ABSTRACT

The yeast *Saccharomyces cerevisiae* contains a pair of paralogous iron-responsive transcription activators Aft1 and Aft2. Aft1 activates the cell-surface iron uptake systems in iron depletion while the role of Aft2 remains poorly understood. This study compares the functions of Aft1 and Aft2 in regulating the transcription of genes involved in iron homeostasis, with reference to the presence/absence of the paralog. Cluster analysis of DNA microarray data identified the classes of genes regulated by Aft1 or Aft2, or both. Aft2 activates the transcription of genes involved in intracellular iron use in the absence of Aft1. Northern blot analyses, combined with chromatin immunoprecipitation experiments on selected genes from each class, demonstrated that Aft2 directly activates the genes *SMF3* and *MRS4* involved in mitochondrial and vacuolar iron homeostasis, while Aft1 does not. Computer analysis found different cis-regulatory elements for Aft1 and Aft2, and transcription analysis using variants of the *FET3* promoter indicated that Aft1 is more specific for the canonical iron-responsive element TGCACCC than is Aft2. Finally, the absence of either Aft1 or Aft2 showed an iron-dependent increase in the amount of the remaining paralog. This may provide additional control of cellular iron homeostasis.

INTRODUCTION

Iron is an essential nutrient but its accumulation can be highly cytotoxic owing to its chemical reactivity, which depends on its redox state (II or III). Prokaryotes and eukaryotes cells have therefore evolved various regulatory mechanisms to control iron homeostasis and so maintain a balance between nutritional deprivation and excess of iron (12, 13). The yeast *Saccharomyces cerevisiae* has two paralogous iron-responsive transcription activators, Aft1 and Aft2, that play key roles in the response to a lack of iron in the environment by increasing the expression of genes involved in iron transport, its sub-cellular distribution and use (28). The N-terminal regions of Aft1 and Aft2, which contain the DNA binding domain (29, 38), are well conserved (3). These N-terminal regions interact with the same DNA promoter *in vitro* (29, 38). The replacement of a conserved cysteine residue in the N-terminal region by phenylalanine makes the gain of function mutant alleles *AFT1-1*^{up} (37) and *AFT2-1*^{up} (29) iron-independent.

Aft1 is located in the cytosol of cells grown under iron-replete conditions but in cells grown under iron-depleted conditions, it is in the nucleus, where it binds to DNA and activates transcription (39). Cells lacking *AFT1* grow poorly under iron-depleted conditions (3, 29, 37). Consistent with this phenotype, Aft1 activates the transcription of genes involved in iron uptake at the plasma membrane. These include genes that encode the high affinity ferrous transport complex composed of the multicopper oxidase (*FET3*) and iron permease (*FTR1*) (1, 34), the copper transporter responsible for delivering copper to Fet3 (*CCC2*) (40), plasma membrane metalloreductases (*FRE1-4*) (5, 10, 41), iron-siderophores transporters (*ARN1-4*) (17, 18, 42, 43) and cell wall mannoproteins, which facilitate the uptake of siderophore-bound iron (*FIT1-3*) (25). Aft1 is also involved in the activation of other genes, such as *FTH1*, that encodes a vacuolar iron transporter (35), and genes with function not yet elucidated in iron metabolism, such as *HMX1*, the homolog of the gene encoding heme oxygenases (26, 33), two members of the *FRE* family (*FRE5-6*) (21) and *CTH2,* a gene recently shown to be involved in mRNA degradation under iron deficiency (27). Others genes were recently shown by DNA microarray

analyses to be regulated by the constitutive *AFT1-1*^{up} mutant allele, but the role of Aft1 in their regulation remains to be elucidated (30, 33).

The role of Aft2 is still unclear, unlike that of Aft1. No phenotype is associated with the lack of *AFT2* alone. Consistent with this lack of phenotype, the genes involved in the iron uptake systems are expressed similarly in the wild type and in the *aft2Δ* mutant ((3) and unpublished results). However, plasmids expressing *AFT2* in the *aft1aft2* mutant activate the transcription of Aft1-target genes in an iron-regulated manner (3, 29). The deletion of *AFT2* exacerbates the phenotype of the *aft1* mutant, rendering the *aft1aft2* double mutant unable to grow under iron-depleted conditions and it abolishes the residual transcription of genes such as *FET3* and *CTH2* that still occurs in the single *aft1* mutant (3, 27). The *aft1aft2* mutant also has many oxidative stress-related phenotypes that are not present in the *aft1* mutant (3). These results suggested that the roles of Aft2 and Aft1 overlap to some extent.

DNA microarray data have defined a set of genes that is activated by the constitutive *AFT2-1*^{up} (29, 30). A few of these genes encode proteins that are involved in iron homeostasis, such as the vacuolar iron transporter *SMF3* (23, 24), the mitochondrial iron transporter *MRS4* (7), and a protein involved in the mitochondrial iron-sulfur cluster assembly, *ISU1* (9, 32). This work was designed to define the involvement of Aft1 and Aft2 in the transcriptional regulation of iron homeostasis, in regard to the presence/absence of the paralog. DNA microarray clustering allowed us to identify several classes of genes that are regulated by Aft1 and/or Aft2, and computer analyses highlighted different consensus sequences for each class. A combination of Northern blotting and chromatin immunoprecipitation experiments with the iron-regulated genes *FET3*, *FTR1*, *SMF3* and *MRS4* demonstrated that the direct transcription activation mediated by either Aft1 or Aft2 is gene-specific and iron-dependent. Aft2 directly activates the transcription of the iron intracellular use genes *SMF3* and *MRS4*, while Aft1 does not. We show that Aft2 functions in the absence of Aft1. We have also obtained evidence that the

amounts of Aft1 and Aft2 are increased in the absence of the paralog, and that iron represses the amounts of Aft1 and Aft2 in these genetic contexts.

MATERIALS AND METHODS

Yeast strains, plasmids and growth conditions

All strains used are listed in Table I. Transcriptome analysis experiments were performed with strains CM3260, Y18 and Y18*aft2Δ*. The strains used for other experiments were derivatives from strains obtained from Research Genetics (Huntsville, AL). The haploid strain SCMC01 (*aft1Δaft2Δ*) was constructed as follows: Y01090 and Y14438 were mated, the diploid strain was selected on medium lacking lysine and methionine and was made to sporulate. Tetrads were dissected out, and spores showing resistance to geneticine and hypersensitivity to copper were characterized: *AFT1* and *AFT2* deletions were verified by PCR, and the known phenotypes of the Y18*aft2*Δ double mutant strain (3) were confirmed. Strains SCMC05 (*AFT2*, *AFT1-HA*), SCMC11, SCMC18 (*AFT1*, *AFT2-HA*), SCMC10 (*aft2*Δ, *AFT1-HA*) and SCMC13 (*aft1*Δ, *AFT2-HA*) carry three tandem copies of the influenza virus hemagglutinin epitope (*HA*) at the very carboxy-terminus of *AFT1* or *AFT2*. The HA epitope tags for *AFT1* and *AFT2* were amplified from the template pFA6a-3HA-HIS3MX6 as described previously (20), using the following primer sets: *AFT1-3HA*: 5'-AATGGTGAACGGCGAGTTGAAGTATGTGAAGCCAGAAGATCGGATCCCCGGGTTAATTAA-3' and 5'-ATGGACGAGAGATACGTCTAAGTTTGATTTCATCTATATGGA-ATTCGAGCTCGTTTAAAC-3'; *AFT2-3HA*: 5'-TGAATTAAATTCTATTGACCCAGCC-TTAATATCAAAATATCGGATCCCCGGGTTAATTAA-3' and 5'-TTAAACGTGATAC-CGTTTTAATGAGTTGAAAACTAAATAAGAATTCGAGCTCGTTTAAAC-3'. The *AFT1-3HA* PCR products were transformed into BY4742 and those of *AFT2-3HA* into BY4741 to generate strains SCMC05 and SCMC11. Strains SCMC18, SCMC10 and SCMC13 were isolated after mating strains SCMC11 and BY4742, SCMC05 and Y01090, and SCMC11 and Y14438, respectively. Epitope tagged strains were verified by PCR, sequencing and protein synthesis. The plasmids pEG202-*AFT1* and pEG202-*AFT2* have been described previously (3). Plasmid pFC-W was kindly provided by Dr Yamaguchi-Iwai; it contains the -263/-234

upstream activation sequence of the *FET3* gene that has been inserted into the *CYC1* promoter and fused to the *LacZ* gene (38). Plasmids pFC-M1, pFC-M2 and pFC-M3 containing site-directed nucleotides substitutions introduced in the *FET3* core sequence (-252/-243) to resemble to the *SMF3* sequence (-362/-353) were constructed as follows : the entire Sal1-BamH1 fragment from the pFC-W was first subcloned into the pUC-18 vector (Stratagene) and the resulting plasmid was used as PCR template for the QuikChange Mutagenesis Kit (Stratagene) according to the manufacturer instructions. The primers used were 5'-GGCTCGACCTTCAAAACCGCACCCATTTGCAGGTGC-3' and its complement for M1 substitutions, 5'-CCTTCAAAAGTGCACCCTGTTGCAGGTGCTCGTCG-3' and its complement for M2 substitutions and 5'-GGCTCGACCTTCAAAACCGCACCCTGTTGC-AGGTGCTCGTCG-3' and its complement for M3 substitutions. Then, the entire Sal1-BamH1 fragment from the pUC-18 vector was re-inserted into the Sal1-BamH1 sites of the pFC-W vector to obtain the pFC-M1, pFC-M2 and pFC-M3 plasmids. All PCR generated sequences were confirmed by DNA sequencing.

All yeast transformations were performed by the lithium acetate method.

The iron-depleted or iron-replete conditions were created by first growing cells at 30°C in a defined medium consisting of an iron-limiting and copper-limiting yeast nitrogen base (Bio101#4027-122) plus 1 μM ferric ammonium sulfate. These cells (OD_{600} = 0.3) were placed in the defined medium with or without 100 μM ferric ammonium sulfate and the cultures were grown for 5 hours to an OD_{600} = 1.0. They were then used for DNA microarray assays, Northern blotting, chromatin immunoprecipitation experiments (ChIP) or β-galactosidase assays.

RNA isolation, Northern analysis and β-Galactosidase Assay

Total RNA extraction, Northern blotting (15 μg total RNA) and hybridization were performed in duplicate, as described previously (14, 31). The ^{32}P-labelled DNA fragments used as probes

corresponded to the open reading frame of each gene. A 1.2-kb *Bam*HI-*Hin*dIII fragment was used for the *ACT1* gene. The 623 bp fragment of *FET3*, the 759 bp fragment of *FTR1*, the 744 bp fragment of *MRS4* and the 924 bp fragment of *SMF3* were obtained by PCR using the primer sets described in Table II. The membranes were exposed for 2 days. Data were quantified using ImageQuant software, and normalized using the *ACT1* mRNA signal. β-Galactosidase was assayed using *o*-nitrophenyl-D-galactopyranoside (11).

Microarray hybridization and analysis

RNA extracted from strains grown exponentially in iron-depleted medium was used to hybridize Yeast GeneFilters® Microarray (Research Genetics, Invitrogen corporation) according to the manufacturer's instructions, except that 5 µg of total RNA were reverse-transcribed. Hybridizations were done in duplicate using two separate sets of filters. Images were acquired after 3 days exposure using a phosphorimager Storm 860 (Molecular Dynamics), and analyzed with the PATHWAYS 3 software (Research Genetics). Those genes previously found to be activated by *AFT1-1*^{up} and/or *AFT2-1*^{up} were selected and subjected to a k-mean clustering (k=5) ((6), http://rana.stanford.edu/clustering). The JavaTreeView program (http://genome-www.stanford.edu/~alok/TreeView) was used to visualize the clustered data. Multiple expectation-maximization for motif elicitation (MEME, (2)) was used to identify shared motifs in the 700 bp of the promoters of similarly regulated genes. Additional information and a version of MEME running on a parallel supercomputer are available at http://www.sdsc.edu/MEME.

Chromatin Immunoprecipitation

Cells were grown exponentially in 100 ml iron-depleted or iron-replete medium to OD_{600} = 1. The chromatin was then prepared (15), and the resulting supernatant volume adjusted to 4 ml before storage at –80°C. Immunoprecipitations were performed in duplicate. 500 µl of the crosslinked chromatin solution was added to 8 µg of anti-HA monoclonal antibodies (Santa Cruz Biotechnology) pre-bound to 10 mg protein A-Sepharose CL-4B (Sigma) and incubated for 1.5 h at room temperature. Protein A-Sepharose CL-4B without antibody was used for background control. Beads were washed twice with 1.6 ml FA-lysis buffer with 500 mM NaCl, once with 1.6 ml 10 mM Tris-HCl pH 8, 0.25 mM LiCl, 1 mM EDTA, 0.5% N-P40, 0.5% sodium deoxycholate, and once with 1.6 ml TE, for 15 min each. Chromatin complexes were released from the beads by incubation in 500 µl 25 mM Tris-HCl pH 7.5, 10 mM EDTA, 0.5% SDS for 15 min at 65°C. Crosslinks from eluates and crude chromatin solution Valencia, CA). (50 µl) were reversed by incubating with 600 µg proteinase K (Sigma) for 1 h at 37°C and overnight at 65°C. The resulting DNA was purified on PCR purification kit columns (Qiagen).

Real-time quantitative PCR analysis

The Qiagen Quantitect SYBR Green PCR Kit was used for quantitative real-time PCR in a LightCycler (Roche Diagnostics). Primer pairs (Table II) were designed with Oligo 4.0-s software to generate products of 90-130 bp. For *FET3*, *SMF3* and *MRS4* promoters, PCR fragments were amplified with primers flanking the iron regulatory sites defined by promoter deletion analyses (23, 30, 38). For the *FTR1* promoter, we designed primers to amplify the region (190 bp) between the two TGCACCC sequences. For *POL1* and *RPO21* used as negatives controls, we designed primers within their coding sequences.

PCR reactions were carried out in 15 µl with 2 µM each primer, and 1x Quantitect SYBR Green PCR Kit. The DNA templates added to the reaction mixture were: $1/150^{th}$ of the immunoprecipitated DNA or the background DNA and $1/50000^{th}$ of the input DNA. The LightCycler run protocol was: denaturation (95°C for 15 min), 45 cycles of amplification and

quantification (95°C for 20 s, 55°C for 20 s, 72°C for 25 s with a single measurement) and melting curve (60-95°C, with heating rate of 0.1°C per second and continuous fluorescence measurement).

Data were analyzed using the Roche LightCycler 3.5 software and the fit point method. The crossing point (CP) was defined as the point at which the fluorescence was 10 times the background fluorescence. The efficiency (E) of each primer pair was calculated from the slope of the linear standard curve ($E = 10^{-1/slope}$) generated with a 5-fold dilution of a DNA input mix. The protein occupancy of each DNA fragment was then calculated as previously described (4): protein occupancy = $(E^{(CP\ input\ -\ CP\ IP\ )})$ / $(E^{(CP\ input\ -\ CP\ bkg)})$. The data were averaged over two independent experiments with real-time PCR performed at least in duplicate (standard deviation is shown by error bars). The fold enrichment of a selected DNA fragment was obtained by dividing the protein occupancy at this DNA fragment by the average protein occupancy at the negative controls (coding sequences of *POL1* and *RPO21*).

Protein extraction and Western blotting

Total protein extracts from 3 ml of cells grown exponentially in iron-depleted or iron-replete media were prepared by the NaOH-TCA lysis technique (36). Aliquots (5 µl) were separated on 8% SDS-PAGE and transferred to nitrocellulose membranes. The membranes were blocked with 3% BSA (Sigma), 0.1% Tween-20 (Sigma) in TBS and probed at room temperature in the same blocking buffer. Anti-HA monoclonal antibodies (Santa Cruz Biotechnology) were diluted at 1:1000 and anti-Pgk1 monoclonal antibodies (Roche Diagnostics) were diluted at 1:5000. Horseradish peroxidase-conjugated anti-mouse immunoglobulin G (diluted 1:1000) was used as the secondary antibody (Sigma) and was detected by enhanced chemiluminescence (ECL kit, Amersham).

RESULTS

Inhibition of the Aft2 regulon by Aft1

We investigated the effects of Aft1 and Aft2 on gene expression under iron-depleted conditions. Previous studies show that the transcription mediated by wild type Aft2 can be detected in the absence of Aft1 (3, 29). We therefore examined the effect of Aft2 on gene expression in an *aft1* mutant genetic context. DNA microarray hybridizations were performed with labeled transcripts extracted from wild type strain, single *aft1* and double *aft1aft2* mutant cells grown in iron-depleted conditions. Comparisons of the gene expression in these genetic contexts allowed us to identify 332 genes whose expression decreased more than 2-fold in at least one of the 3 comparisons wt/*aft1*, wt/*aft1aft2* or *aft1*/*aft1aft2* (Experimental data sets are available at GEO, http://www.ncbi.nlm.nih.gov/geo/, accession number GSE1763). In order to take advantage of both our "loss of function" approach and previous "gain of function" analyses, we combined the experimental data and focused on those 50 genes that were postulated as potential targets of *AFT1-1*^{up} and/or *AFT2-1*^{up} (29, 30, 33). Genes with similar transcription profiles were grouped by cluster analysis into 5 classes (A to E, Fig. 1).

Class A contained those genes whose mRNAs were at least 2-fold more abundant in wild type than in either the *aft1* or the *aft1aft2* mutants. Most of these genes had been shown to be Aft1-target genes, encoding proteins involved in the plasma membrane iron transport (*e.g.: FET3*, *FRE1*, *FIT2-3,* and *ARN1-4*). Class B contained genes whose mRNAs amounts in the single *aft1* mutant were similar to those of the wild type strain, but whose mRNAs amounts were lower in the *aft1aft2* double mutant. This transcription profile suggests that the roles of Aft1 and Aft2 overlap in the control of these genes. Class B, like class A, contained genes involved in iron metabolism, except for *ZRT1* that encodes the high affinity zinc transporter (44). Surprisingly, the mRNAs of class C and D genes were more abundant in the *aft1* mutant than in the wild type, indicating that Aft1 has a negative influence on the transcription of these genes. The class C and D genes showed more mRNAs in the *aft1* mutant than in the double mutant

(positive *aft1/aft1aft2* ratio), as did those of class B, suggesting that Aft2 activates their transcription in the absence of Aft1. As shown in Figure 1, most of the class C and D genes are activated by *AFT2-1*^{up} (29, 30). These genes had almost the same transcription profiles, except that the class C genes had a higher wild type/*aft1aft2* ratio than did those of class D. Unlike classes A and B, classes C and D contained few genes encoding proteins involved in iron homeostasis. **T**hese genes take no part in iron transport across the plasma membrane, but are involved in vacuolar iron transport (*SMF3*, *FTH1*, *FET5*) or mitochondrial iron transport and use (*MRS4*, *ISU1*). Lastly, class E contained genes with neither positive wild type/*aft1* nor positive *aft1*/*aft1aft2* ratios, unlike those of A-D. This suggests that Aft1 or Aft2 are not important for their transcription under our experimental conditions, and the effects of Aft1 and Aft2 on their transcription were not investigated further.

The MEME program (2) was used to identify potential regulatory elements in the promoters of the genes regulated by Aft1 and Aft2. The promoter region between the predicted ATG start codon and 700 bp upstream was chosen to identify the most probable motif within each class A-E of input promoters (Fig. 1-2). MEME successfully identified the canonical iron-responsive element (38) TGCACCC in the promoters of the A and B class genes (Fig. 2). Thus 13 of the 19 genes (68%) analyzed contained at least one copy of this sequence in either orientation. Analysis of the whole genome identified 3% of all open reading frames having this sequence within their promoter. There was also generally an A 2 bases upstream of the TGCACCC sequence. In contrast, the sequence TGCACCC was present in only 6 of the 22 class C and D gene promoters (27%). The most probable motif identified within the promoters of class C and D genes was restricted to G/ACACCC, with 20 of the 22 genes (91%) containing at least one copy of this motif. This sequence was present in 24% of the promoters of the whole genome. About 80% of the class C genes contained the G/ACACCC sequence followed by an AT-rich region starting 3 bases downstream the motif. MEME identified the GCACCCT sequence as the most probable motif of the class E genes; it was present in 44% of the genes analyzed (4 of

9 genes) and in 3.2% of the promoters of the whole genome. This sequence was often preceded by a T, reminiscent of the known TGCACCC sequence.

We attempted to distinguish between the direct and indirect effects of Aft1 and Aft2 on the regulation of classes A-B-C-D genes by examining one iron-regulated gene from each class using ChIP experiments and Northern blotting analyses. The *FET3*, *FTR1*, *SMF3* and *MRS4* genes were chosen arbitrarily because of their known function in iron homeostasis. The ChIP experiments were performed in two genetic contexts (presence and absence of the paralogous protein) because Aft1 and Aft2 could interfere with each other.

Direct activation of FET3 transcription by Aft1, but not by Aft2

In vivo DNA footprint analyses have shown that Aft1 binds to the *FET3* FeRE sequence and activates its transcription in an iron-dependent manner (37, 38). In contrast, the role of Aft2 in the transcriptional activation of *FET3* is not clear: Aft2 binds to the same *FET3* FeRE sequence as Aft1 *in vitro* (29), but Aft2-dependent regulation of *FET3 in vivo* has only been reported for specific conditions such as overexpression of *AFT2* in the absence of Aft1 (3) or expression of the constitutive allele *AFT2-1*^{up} (29, 30). Northern blot analyses (Fig. 3A) confirmed that the transcription of *FET3* required *AFT1* but not *AFT2* (3). Overexpression of *AFT2* in *aft1*Δ*aft2*Δ increased the amount of *FET3* mRNAs, although this was still lower than that resulting from overexpression of *AFT1*. The amount of *FET3* mRNAs increased 1.5-fold in the absence of Aft2. ChIP analyses showed that Aft1 was strongly bound to the *FET3* promoter in wild type cells whereas Aft2 was not (Fig. 3B). The occupancy of the *FET3* promoter by Aft1 also increased 1.3-fold in the absence of Aft2. Conversely, low but reproducible amounts of Aft2 were bound to the *FET3* promoter in the absence of Aft1, although this appeared to be insufficient to sustain observable *FET3* mRNAs production (Fig. 3A-B). We further investigated the effect of iron on *FET3* transcription and on the binding of Aft1/Aft2 to the *FET3* promoter. Transcription of *FET3* was repressed by adding iron (Fig. 3C), as previously reported (37). However, residual *FET3* mRNAs were still detected in wild type and *aft2*Δ

strains. ChIP assays indicated that iron decreased Aft1 binding to the *FET3* promoter 5-fold, but it was still 4 to 5-fold higher than the binding to non-relevant DNA controls (Fig. 3D). The weak binding of Aft2 to the *FET3* promoter in the absence of Aft1 was repressed by iron. Thus, Aft2 does not activate the transcription of *FET3*, although it can poorly bind to the *FET3* promoter in the absence of Aft1, and *FET3* is specifically activated by Aft1 under iron-depletion.

Direct activation of FTR1 transcription by Aft2 in the absence of Aft1

FTR1 is an Aft1-target gene (38), and its transcription is reportedly activated by the *AFT2-1*^{up} mutant allele (29), albeit to a lower degree than by *AFT1-1*^{up} (30). Our DNA microarray results suggested that Aft1 and Aft2 were redundant in the activation of *FTR1* transcription (Fig. 1). Northern blot analyses confirmed the DNA microarray data: the amounts of *FTR1* mRNAs in wild type, *aft1*Δ and *aft2*Δ strains were similar, while no transcript was detected in the *aft1*Δ*aft2*Δ double mutant (Fig. 4A). Overexpression of *AFT2* induced the expression of *FTR1* but to a lesser extent than overexpression of *AFT1*, in agreement with previous DNA microarray data obtained with the constitutive *AFT1-1*^{up}/ *AFT2-1*^{up} alleles (29, 30, 33). ChIP experiments showed that Aft1 was bound to the *FTR1* promoter in wild type and *aft2*Δ strains in iron-depleted conditions (Fig. 4B). The Aft1 occupancy of the *FTR1* promoter was increased 2-fold in the absence of Aft2. Aft2 was also bound to the *FTR1* promoter, but only in the absence of Aft1. Aft1 and Aft2 occupied the *FTR1* promoter similarly in the absence of their paralog, consistent with the similar amounts of *FTR1* mRNAs found in the *aft1*Δ and *aft2*Δ mutants (Fig. 3A and Fig. 3B). These analyses indicate that Aft2 can compensate for the absence of Aft1 in the direct control of *FTR1* transcription. We also investigated the effect of iron on the Aft1- and Aft2-dependent regulation of *FTR1*. The transcription of *FTR1* decreased in iron-replete conditions, as previously reported (38). However, there was still residual transcription of *FTR1* in the wild type and *aft2*Δ strains, but not in the *aft1*Δ mutant (Fig. 4C). The degree of *FTR1* promoter occupancy by Aft1 was 2 to 4-fold lower than under iron-

depleted conditions, but it was still 2-fold higher than for DNA controls, whereas occupancy of the *FTR1* promoter by Aft2 in the *aft1*Δ mutant was 7-fold lower, reaching that of the DNA controls (Fig. 4D). Therefore, the binding of Aft2 to the *FTR1* promoter is more sensitive to iron than is the binding of Aft1.

Opposing roles for Aft1 and Aft2 in the control of SMF3 and MRS4

The transcription of *SMF3* is activated by iron starvation in an Aft1/Aft2 dependent manner (23). Previous DNA microarray analyses indicated that this transcription is activated by *AFT2-1*^{up} and, to a lesser extent, by *AFT1-1*^{up} (29, 30, 33). However, *SMF3* may be controlled by other transcription factors, unlike *FET3* and *FTR1,* because its transcription is not abolished in the *aft1*Δ*aft2*Δ mutant (23). Our DNA microarray analysis indicated that the amount of *SMF3* mRNAs in *aft1*Δ was greater than in wild type, although it was lower than in wild type in *aft1*Δ*aft2*Δ (Fig. 1). Northern blot analyses and ChIP experiments were performed to elucidate the antagonistic effect of the *AFT1* deletion in wild type *versus aft2*Δ genetic contexts. The amount of *SMF3* mRNAs in the *aft1*Δ mutant was higher than in the wild type, consistent with the DNA microarray data, while it was slightly lower than in the wild type in the *aft2*Δ mutant (Fig. 5A). The effect of the *AFT2* deletion was epistatic on that of the *AFT1* deletion since the amount of *SMF3* mRNAs in the double *aft1*Δ*aft2*Δ mutant was lower than in the wild type strain. The signal still detected in *aft1*Δ*aft2*Δ confirmed that other factors are involved in the activation of *SMF3* transcription. Finally, overexpression of either *AFT1* or *AFT2* in the *aft1*Δ*aft2*Δ mutant clearly induced *SMF3* expression. The occupancy of the *SMF3* promoter by Aft1 was only 1.8-fold greater than in the DNA controls in *aft2*Δ and 2.7-fold greater than in the DNA controls in the wild type strain (Fig. 5B). In contrast, a great deal of Aft2 (12 times more than in the DNA controls) was bound to the *SMF3* promoter in the absence of Aft1. No Aft2 was bound to the *SMF3* promoter in wild type cells, as for *FET3* and *FTR1*. This suggests that the increased *SMF3* mRNAs in *aft1*Δ was due to the direct binding of Aft2 and its activation of transcription. We checked this by investigating the Aft1-dependent and Aft2-

dependent transcription of *SMF3* in the presence of iron. The experiments performed in iron-replete conditions showed correlated decreases in both the amounts of *SMF3* mRNAs (3-fold) and the occupancy of the *SMF3* promoter by Aft2 in the *aft1*Δ mutant (5-fold) (Fig. 5C and 5D). It also showed that the low occupancy of the *SMF3* promoter by Aft1 was affected by iron. We conclude that Aft2 directly activates the transcription of *SMF3* when Aft1 is absent.

DNA microarray analyses have shown that the transcription of *MRS4* is activated by *AFT2-1*^{up} (29) and *AFT1-1*^{up}, but to a lower degree (30). However, in contrast to the positive action of Aft1 in the control of *MRS4,* others have reported that *MRS4* transcription is greater in the *aft1*Δ mutant than in the wild type strain (7). Our DNA microarray data (Fig. 1) and Northern blot analyses (Fig. 6A) confirmed the latter result. Moreover, the introduction of a plasmid carrying *AFT1* into the *aft1*Δ mutant led to a decrease in the *MRS4* mRNAs (Fig 6A). The amount of *MRS4* mRNAs was not affected by sole deletion of *AFT2*, but the increased amount of *MRS4* mRNAs in the *aft1*Δ mutant was suppressed by deleting *AFT2* as well. The remaining signal in the *aft1*Δ*aft2*Δ mutant indicated that other factors are involved in activating *MRS4* transcription. These results suggest that the increased transcription of *MRS4* in the *aft1*Δ mutant is due to Aft2, as for *SMF3*. Considerable amounts of Aft2 were consistently bound to the *MRS4* promoter in the absence of Aft1 (27.5-fold more than to the DNA controls) (Fig. 6B). Little Aft2 was bound to the *MRS4* promoter in wild type cells (2-times more than bound to the DNA controls). No Aft1 was bound to the *MRS4* promoter in wild type or in *aft2*Δ strains, unlike Aft2. The amounts of *MRS4* mRNAs were greatly reduced in the absence of Aft1 under iron-replete conditions (Fig. 6C). In agreement with this decreased *MRS4* mRNAs amount, the binding of Aft2 to the *MRS4* promoter was 15-times less than under iron limitation (Fig. 6D). Thus, Aft2 directly activates the transcription of *MRS4* in iron-depleted conditions when Aft1 is absent. Control experiments indicated that there was no binding of Aft2 in a wild type strain grown with iron, whatever the promoter studied (*FET3*, *FTR1*, *SMF3*, *MRS4*) (data not shown).

Mutational analysis of the FET3 regulatory sequence

The above results indicate that Aft1 and Aft2 activate different target genes. The transcription of *FET3* was specifically activated by Aft1 while those of *SFM3* and *MRS4* were specifically activated by Aft2. Furthermore, computer analyses (Fig.2) identified slight difference between the consensus binding sites of genes activated by either Aft1 (TGCACCC) or Aft2 (G/ACACCC). We modified the iron regulatory sequence in the *FET3* promoter to resemble that of the *SFM3* promoter by site-directed mutagenesis so as to investigate the functional importance of the difference in these consensus binding sites. Di-nucleotides in 5' or/and 3' of the core sequence GCACCC of the pFC-W *FET3* promoter Lac Z fusion were changed as described in Fig.7A. The pFC-W plasmid and the plasmids pFC-M1, pFC-M2, pFC-M3 with mutated-promoter were used to transform the wild type, *aft1*Δ, *aft2*Δ, and *aft1*Δ*aft2*Δ strains. These plasmids were also used to transform the *aft1*Δ*aft2*Δ strain harbouring a high copy number plasmid which over-expressed either *AFT1* or *AFT2*. We evaluated the Aft1 and Aft2 transcriptional activity from the mutated promoters by comparing the β-galactosidase activities in these strains. The β-galactosidase activities obtained with the pFC-W plasmid in the different genetic contexts (Fig.7B) confirmed previous data showing that the transcription of *FET3* is predominantly Aft1-dependent (3). The slightly higher β-galactosidase activity in *aft2*Δ than in the wild type strain is in agreement with the increased *FET3* mRNA (Fig.3A). The β-galactosidase activity obtained with the pFC-M1 was 3.5-fold lower than that obtained with the pFC-W plasmid in the wild type strain, 2.5-fold lower with pFC-M2 and 6.6-fold lower with pFC-M3. Similar results were obtained in the *aft2*Δ strain. These results indicate that Aft1 is a poor activator for the mutated promoters and that Aft2 is not involved in the residual activation when Aft1 is present. No significant β-galactosidase activity was detected in the *aft1*Δ*aft2*Δ mutant transformed with the pFC-W, pFC-M1, pFC-M2 or pFC-M3 plasmids, indicating that the β-galactosidase activity mediated by these plasmids was strictly Aft1/2-dependent. The β-galactosidase activity measured in the *aft1*Δ mutant, attributed to Aft2, was

3.5-fold higher than that of the *aft1*Δ*aft2*Δ mutant with the pFC-W. The Aft2-dependent activation was more efficient in the pFC-M1 context (2.3-fold greater than pFC-W); in contrast, this Aft2-dependent activation was lower (1.7-fold decrease) with pFC-M2 than with pFC-W, and remained unchanged with pFC-M3. The β-galactosidase activities measured with the pFC-W, pFC-M1, pFC-M2 or pFC-M3 were decreased 3 to 4 fold by adding 100 μM iron in the wild type, *aft2*Δ and *aft1*Δ strains (data not shown). The differences in Aft1- and Aft2-dependent activation were further confirmed with *aft1*Δ*aft2*Δ strains over-expressing either the *AFT1* or *AFT2* gene (Fig 7B). Over-expression of *AFT2* increased the transcription from the pFC-M1 promoter 2.4-fold and from the pFC-M3 promoter 2.6-fold, while it decreased the transcription from pFC-M2 1.9-fold compared to the pFC-W. The transcription from the pFC-M1, pFC-M2 and pFC-M3 was lower than with the pFC-W when *AFT1* was over-expressed.

Iron dependent increases in Aft1 and Aft2 in the absence of the paralog

The above results show that the occupancy of promoters by Aft1 and Aft2 depends on the presence or the absence of the paralog and on the iron concentration in the culture medium. We measured the total Aft1-HA and Aft2-HA levels in wild type and in either *aft2*Δ or *aft1*Δ cells grown in iron-depleted and in iron-replete conditions by Western blotting with anti-HA antibody to determine whether these effects resulted from changes in the amounts of Aft1 and Aft2 proteins. The concentration of Aft1 was higher in the absence of Aft2 than in the wild type under iron-depletion (Fig 8A); this is in agreement with the increased Aft1-mediated activation of *FET3* and *FTR1* transcription in the *aft2*Δ strain (Fig. 3-4). The amount of Aft1 in wild type cells was not greatly affected by adding iron, consistent with previous analyses (39). Nevertheless, it was decreased at least 2-fold by iron in the absence of Aft2. Analysis of the amounts of Aft2 showed a weak band corresponding to Aft2, fainter than that of Aft1 in wild type cells (Fig. 8B). The amount of Aft2 was 3.3-fold higher in the absence of Aft1 under iron-depleted conditions, in agreement with the stimulation of the Aft2-activated transcription alone

under these conditions (Fig. 3-6). The amount of Aft2 in wild type cells was not affected by adding iron while it was decreased by iron in the absence of the paralog, as was Aft1. The Western blot analyses therefore show that the amounts of Aft1 and Aft2 are increased in the absence of the paralog under iron-depletion, and that iron represses the amounts Aft1 and Aft2 in these genetic contexts.

DISCUSSION

The yeast paralogs, Aft1 and Aft2, are iron-responsive transcription activators that have overlapping, but not redundant, functions in iron homeostasis. Aft1 is the major regulator of the iron uptake systems, while the role of Aft2 is not yet clear. We assessed the role of Aft2 by analyzing the profiles of gene expression in the wild type yeast strain and in mutant strains deficient for Aft1 or for both Aft1 and Aft2. The cells were grown in iron-depleted medium, which promotes Aft1 and Aft2 dependent activation of the genes involved in iron metabolism. We used our DNA microarray data to perform a cluster analysis on the 50 genes that were previously identified as target genes of the *AFT1-1*^{up} and/or *AFT2-1*^{up} alleles (29, 30, 33). This allowed us to uncover several classes of genes that are differentially regulated by Aft1 and Aft2. The classes A-D genes exhibited transcription profiles that were consistent with a role of either Aft1 (class A), Aft2 (classes C and D), or both (class B), in their activation. Only the small class E genes exhibited no transcription decrease in each of the 3 comparisons wt/*aft1*, wt/*aft1aft2* or *aft1/af1aft2*. This discrepancy between our "loss of function" analyses and the previous "gain of function" results could be caused by the different genetic contexts or different experimental conditions.

The detailed study by Northern blotting and ChIP experiments of the prototype genes *FET3*, *FTR1*, *SMF3* and *MRS4*, representing the four A, B, C and D classes genes, respectively, has provided new insights into the direct and indirect actions of Aft1 and Aft2 in the regulation of genes involved in iron homeostasis. The degrees of promoter occupancy by Aft1 and Aft2 were correlated with the subsequent transcription of the corresponding genes. A striking feature here is that Aft1 and Aft2 mostly activate distinct iron-regulated genes *in vivo* by selective binding to the promoter, while they are able to bind to the same sequence *in vitro* (29). Aft1 binds well to *FET3* and *FTR1* promoters and poorly to the *SMF3* promoter, but Aft1 is not bound to the *MRS4* promoter; conversely, Aft2 binds poorly to the *FET3* promoter, and well to the *FTR1*, *SMF3* and *MRS4* promoters (summarized in Fig. 9A). This raises the question of how Aft1 and

Aft2 identify the appropriate promoters. A search for specific cis-acting sequences in the promoter regions of class A and B genes activated by Aft1 identified the canonical TGCACCC sequence of the defined FeRE element (38), indicating the importance of this sequence in the Aft1-mediated activation. In contrast, we observed that the consensus sequence in the promoter regions of genes specifically activated by Aft2 (classes C and D) was not the TGCACCC sequence, but the shorter G/ACACCC sequence (Fig.2). Hence, the TGCACCC sequence appears to be important for Aft1-mediated activation, but not for Aft2-mediated activation. This was confirmed by transcriptional analysis of a LacZ reporter gene cloned under the control of variants of the *FET3* GTGCACCCAT iron responsive element. Changing the 5' GT to CC dramatically decreased Aft1-dependent activation. Changing the 3' AT to TG also affected the Aft1-mediated activation by decreasing the transcription of LacZ, but to a lesser extent than the previous mutation. Introducing both changes in the 5' and 3' of the *FET3* iron responsive element led to a cumulated loss of Aft1-mediated transcription. By contrast with Aft1 reactivity, the 5' variant *FET3* CCGCACCCAT element supported increased Aft2-mediated activation. Although the activation measured with the natural amount of Aft2 was low, it was significant, and over-expression of *AFT2* confirmed that this 2bp change is critical for increased activation. Changing only the 3' end of the site (AT to TG) decreased the Aft2-mediated activation. The two mutations led to an overall increased activation when *AFT2* was over-expressed. Our results on Aft1 mediated activation agree well with previous DNA binding competition experiments demonstrating that the *in vitro* translated Aft1 protein interacted better with the TGCACCCA sequence than with the sequences GGCACCCA or TGCACCCC (38). The new data we provided on Aft2 mediated activation are also in accordance with *in vivo* analyses of *lacZ* reporter fusion constructs showing (1) that iron-regulation of the Aft2 activated gene *SMF3* depends on the $^{-361}$CGCACCC sequence and not on the $^{-430}$TGCACCC sequence (22) and (2) that the *AFT2-1^{up}* allele activates the transcription of *MRS4* through the $^{-238}$GGCACCC sequence (30). Taken together, our computer analysis of the iron responsive

elements of the Aft1 and Aft2 regulated genes and transcriptional analysis of the *FET3* promoter LacZ fusion provide strong support for differently defined Aft1 and Aft2 DNA binding sites; Aft1 appears to be more selective in recognising the 5' context of the GCACCC sequence than is Aft2. However, the presence of the TGCACCC sequence in the promoter region of a gene is not sufficient for its activation by Aft1 because some class C, D and E genes contain the TGCACCC sequence in their promoter regions and are not activated by Aft1 (Fig.1-2). Thus, Aft1 (and Aft2) may recognize the promoter through combination with other trans-acting factors, in addition to specific regulatory cis-acting sequence. Recent studies have shown that the HMG-box chromatin-associated architectural factor Nhp6 associates with Aft1 *in vivo* to facilitate its recruitment to the promoter region of certain of the Aft1-activated genes (8).

Our results show that Aft1 specifically activates *FET3* transcription and that Aft2 specifically activates *SMF3*/*MRS4* transcription (Fig 3-5-6). In contrast, the constitutive allele *AFT1-1*^{up} activates the transcription of *MRS4* (30) and *AFT2-1*^{up} activates that of *FET3* (29, 30). The discrepancy between these results suggests that strains carrying the *AFT1*/*AFT2* wild type alleles are required to unravel the specificity of gene targeting by Aft1 and Aft2, and that the expression of one hyperactive *AFT1-1*^{up}/ *AFT2-1*^{up} allele may lead to aberrant activation of genes specifically controlled by the paralog. More importantly, the specificity of gene activation by Aft1 and Aft2 described in this work correlates with a specificity of gene function: Aft1 activates specifically the transcription of genes involved in cell-surface iron uptake systems (*FET3*, *FRE1*, *ARN1-4* and *FIT2-3*, Fig.1, class A) while Aft2 activates specifically the transcription of genes involved in vacuolar and mitochondrial iron sub-compartimentation and use (*SMF3*, *FRE6*, *FTH1*, *MRS4*, *FET5* and *ISU1*, Fig. 1 classes C and D). Thus, with two paralogous transcription factors displaying a functional specialization in the control of iron homeostasis, the cell may adapt to environmental iron changes with greater flexibility.

Phenotype analyses have shown that the sole *AFT2* deletion confers no iron-specific phenotype, whereas it reveals mis-regulation of intracellular iron use and oxidative stress-related phenotypes in the absence of Aft1 (3). Consistently, we have now shown that the Aft2-mediated activation of transcription is revealed under iron-depleted conditions and in the absence of Aft1. This suggests that the Aft2 activity is triggered by exacerbated iron-limiting conditions caused by the cumulative effects of environmental iron depletion and a lack of Aft1-dependent iron uptake systems. Thus, in response to severe iron-limitation, the activation by Aft2 of the transcription of genes involved in vacuolar and mitochondrial iron transport may lead to a re-organization of the intracellular iron distribution. This is further supported by recent data indicating that the Aft2-target gene *MRS4* is involved in a mitochondrial-vacuolar iron-signaling pathway (19). A hierarchical model implicating Aft1 and Aft2 in a graded response to iron-limitation fits well with the greater sensitivity of Aft2 to iron: a given iron concentration in the culture medium may completely abolish the binding of Aft2 to DNA, but only decrease that of Aft1. Further investigation is now required to clarify the fine-tuning of Aft2 triggering in response to iron-limitation.

The absence of one of the Aft1/Aft2 paralogs under iron-deprivation conditions leads to an increase in the binding of the resident paralog to its specific promoters and subsequent gene activation (Fig. 3-6). These effects are correlated with a change in the abundance of paralog protein in whole cells (Fig. 8 and diagram in Fig. 9B). The extent to which the absence of either Aft1 or Aft2 increases the amount of the remaining paralog protein varies: the Aft2 concentration increases more in the absence of Aft1 than does that of Aft1 in the absence of Aft2. The reciprocal negative influence of Aft1 and Aft2 may reflect a compensatory mechanism to counterbalance a failure in processes regulated by one factor by stimulating those of the paralog. This would allow the cell to tightly coordinate the Aft1-mediated regulation of extracellular iron transport and the Aft2-mediated regulation of iron intracellular use.

The modulations of proteins amounts may involve transcriptional and/or post-transcriptional regulation. Aft1 binds to its own promoter (16). We found a $^{-614}$TGCACCC and a $^{-658}$GGCACCC sequence in the *AFT1* promoter. This suggests that Aft1 and Aft2 are directly involved in the regulation of *AFT1* transcription. In contrast, no CACCC core element of the FeRE sequence was found in the *AFT2* promoter. Any change in its transcription in response to *AFT1* deletion would thus occur through other cis- and trans-regulatory elements. Post-translational effects may also be involved. Our data agree with recent work on mammals showing that the amount of the iron-regulatory protein IRP2 is increased when the paralog gene encoding IRP1 is deleted. Since iron regulates IRP2 by mediating its proteasomal degradation, these experiments suggest that IRP1 is involved in this step of regulation (22). We show that the negative effect of Aft1 and Aft2 on the amount of the paralog is iron-dependant. How iron is involved in controlling the balance between the Aft1 and Aft2 proteins is still unknown and answering this question is critical for a better understanding of the functions of these iron-responsive paralogous transcription factors in the yeast cell. Iron regulates the function of Aft1 by modulating its sub-cellular distribution (39), but is likely to be involved at other steps of Aft1 control. Nothing is yet known about the regulation of Aft2 function by iron. As a first step towards clarifying this critical point, experiments are in progress to determine the level at which iron regulates Aft2 abundance in the absence of Aft1.

ACKNOWLEDGEMENTS

We thank Joel Pothier, Laurent Kuras, Arnaud Teichert and Renata Santos for helpful discussions and all the members of Rosine Haguenauer-Tsapis's laboratory for advice and technical support. Frederic Devaux critically reads the manuscript. The English text was edited by Dr Owen Parkes. This work was supported by grants from the Ministère de la Recherche (Programme de Recherches Fondamentales en Microbiologie, Maladies Infectieuses et Parasitaires) and the Association pour la Recherche sur le Cancer (ARC n° 5439).

REFERENCES

1. **Askwith, C., D. Eide, A. Van Ho, P. S. Bernard, L. Li, S. Davis-Kaplan, D. M. Sipe, and J. Kaplan.** 1994. The *FET3* gene of *S. cerevisiae* encodes a multicopper oxidase required for ferrous iron uptake. Cell **76:**403-410.

2. **Bailey, T. L., and C. Elkan.** 1994. Fitting a mixture model by expectation maximization to discover motifs in biopolymers. Proc. Int. Conf. Intell. Syst. Mol. Biol. **2:**28-36.

3. **Blaiseau, P. L., E. Lesuisse, and J. M. Camadro.** 2001. Aft2p, a novel iron-regulated transcription activator that modulates, with Aft1p, intracellular iron use and resistance to oxidative stress in yeast. J. Biol. Chem. **276:**34221-34226.

4. **Cobb, J. A., L. Bjergbaek, K. Shimada, C. Frei, and S. M. Gasser.** 2003. DNA polymerase stabilization at stalled replication forks requires Mec1 and the RecQ helicase Sgs1. EMBO J. **22:**4325-4336.

5. **Dancis, A., R. D. Klausner, A. G. Hinnebusch, and J. G. Barriocanal.** 1990. Genetic evidence that ferric reductase is required for iron uptake in *Saccharomyces cerevisiae*. Mol. Cell. Biol. **10:**2294-2301.

6. **Eisen, M. B., P. T. Spellman, P. O. Brown, and D. Botstein.** 1998. Cluster analysis and display of genome-wide expression patterns. Proc. Natl. Acad. Sci. USA **95:**14863-14868.

7. **Foury, F., and T. Roganti.** 2002. Deletion of the mitochondrial carrier genes *MRS3* and *MRS4* suppresses mitochondrial iron accumulation in a yeast frataxin-deficient strain. J. Biol. Chem. **277:**24475-24483.

8. **Fragiadakis, G. S., D. Tzamarias, and D. Alexandraki.** 2004. Nhp6 facilitates Aft1 binding and Ssn6 recruitment, both essential for FRE2 transcriptional activation. EMBO J. **23:**333-342.

9. **Garland, S. A., K. Hoff, L. E. Vickery, and V. C. Culotta.** 1999. Saccharomyces cerevisiae ISU1 and ISU2: members of a well-conserved gene family for iron-sulfur cluster assembly. J. Mol. Biol. **294:**897-907.

10. **Georgatsou, E., and D. Alexandraki.** 1999. Regulated expression of the Saccharomyces cerevisiae Fre1p/Fre2p Fe/Cu reductase related genes. Yeast **15:**573-584.

11. **Guarente, L.** 1983. Yeast promoters and lacZ fusions designed to study expression of cloned genes in yeast. Methods Enzymol. **101:**181-191.

12. **Hantke, K.** 2001. Iron and metal regulation in bacteria. Curr. Opin. Microbiol. **4:**172-177.

13. **Hentze, M. W., M. U. Muckenthaler, and N. C. Andrews.** 2004. Balancing acts: molecular control of mammalian iron metabolism. Cell **117:**285-297.

14. **Kohrer, K., and H. Domdey.** 1991. Preparation of high molecular weight RNA. Methods Enzymol. **194:**398-405.

15. **Kuras, L., and K. Struhl.** 1999. Binding of TBP to promoters in vivo is stimulated by activators and requires Pol II holoenzyme. Nature **399:**609-613.

16. **Lee, T. I., N. J. Rinaldi, F. Robert, D. T. Odom, Z. Bar-Joseph, G. K. Gerber, N. M. Hannett, C. T. Harbison, C. M. Thompson, I. Simon, J. Zeitlinger, E. G. Jennings, H. L. Murray, D. B. Gordon, B. Ren, J. J. Wyrick, J. B. Tagne, T. L. Volkert, E. Fraenkel, D. K. Gifford, and R. A. Young.** 2002. Transcriptional regulatory networks in Saccharomyces cerevisiae. Science **298:**799-804.

17. **Lesuisse, E., P. L. Blaiseau, A. Dancis, and J. M. Camadro.** 2001. Siderophore uptake and use by the yeast *Saccharomyces cerevisiae*. Microbiol. **147:**289-298.

18. **Lesuisse, E., M. Simon-Casteras, and P. Labbe.** 1998. Siderophore-mediated iron uptake in *Saccharomyces cerevisiae*: the *SIT1* gene encodes a ferrioxamine B permease that belongs to the major facilitator superfamily. Microbiol. **144:**3455-3462.

19. **Li, L., and J. Kaplan.** 2004. A mitochondrial-vacuolar signaling pathway in yeast that affects iron and copper metabolism. J. Biol. Chem. **279:**33653-33661.

20. **Longtine, M. S., A. McKenzie, 3rd., D. J. Demarini, N. G. Shah, A. Wach, A. Brachat, P. Philippsen, and J. R. Pringle.** 1998. Additional modules for versatile and economical PCR-based gene deletion and modification in Saccharomyces cerevisiae. Yeast **14:**953-961.

21. **Martins, L. J., L. T. Jensen, J. R. Simon, G. L. Keller, D. R. Winge, and J. R. Simons.** 1998. Metalloregulation of FRE1 and FRE2 homologs in Saccharomyces cerevisiae. J. Biol. Chem. **273:**23716-23721.

22. **Meyron-Holtz, E. G., M. C. Ghosh, K. Iwai, T. LaVaute, X. Brazzolotto, U. V. Berger, W. Land, H. Ollivierre-Wilson, A. Grinberg, P. Love, and T. A. Rouault.** 2004. Genetic ablations of iron regulatory proteins 1 and 2 reveal why iron regulatory protein 2 dominates iron homeostasis. EMBO J. **23:**386-395.

23. **Portnoy, M. E., L. T. Jensen, and V. C. Culotta.** 2002. The distinct methods by which manganese and iron regulate the Nramp transporters in yeast. Biochem. J. **362:**119-124.

24. **Portnoy, M. E., X. F. Liu, and V. C. Culotta.** 2000. Saccharomyces cerevisiae expresses three functionally distinct homologues of the nramp family of metal transporters. Mol. Cell. Biol. **20:**7893-7902.

25. **Protchenko, O., T. Ferea, J. Rashford, J. Tiedeman, P. O. Brown, D. Botstein, and C. C. Philpott.** 2001. Three cell wall mannoproteins facilitate the uptake of iron in *Saccharomyces cerevisiae*. J. Biol. Chem. **276:**49244-49250.

26. **Protchenko, O., and C. C. Philpott.** 2003. Regulation of intracellular heme levels by HMX1, a homologue of heme oxygenase, in Saccharomyces cerevisiae. J. Biol. Chem. **278:**36582-36587.

27. **Puig S., Askeland E., Thiele DJ.** 2005. Coordinated remodeling of cellular metabolism during iron deficiency through targeted mRNA degradation. Cell **120:**99-110.

28. **Rutherford, J. C., and A. J. Bird.** 2004. Metal-responsive transcription factors that regulate iron, zinc, and copper homeostasis in eukaryotic cells. Eukaryot. Cell. **3:**1-13.

29. **Rutherford, J. C., S. Jaron, E. Ray, P. O. Brown, and D. R. Winge.** 2001. A second iron-regulatory system in yeast independent of Aft1p. Proc. Natl. Acad. Sci. USA **98:**14322-14327.

30. **Rutherford, J. C., S. Jaron, and D. R. Winge.** 2003. Aft1p and Aft2p mediate iron-responsive gene expression in yeast through related promoter elements. J. Biol. Chem. **278:**27636-27643.

31. **Sambrook, J., E. F. Fritsch, and T. Maniatis.** 1989. Molecular cloning: a laboratory manual, 2nd ed. Cold Spring Harbor Laboratory, Cold Spring Harbor, N.Y.

32. **Schilke, B., C. Voisine, H. Beinert, and E. Craig.** 1999. Evidence for a conserved system for iron metabolism in the mitochondria of *Saccharomyces cerevisiae*. Proc. Natl. Acad. Sci. USA **96:**10206-10211.

33. **Shakoury-Elizeh, M., J. Tiedeman, J. Rashford, T. Ferea, J. Demeter, E. Garcia, R. Rolfes, P. O. Brown, D. Botstein, and C. C. Philpott.** 2004. Transcriptional remodeling in response to iron deprivation in Saccharomyces cerevisiae. Mol. Biol. Cell. **15:**1233-1243.

34. **Stearman, R., D. S. Yuan, Y. Yamaguchi-Iwai, R. D. Klausner, and A. Dancis.** 1996. A permease-oxidase complex involved in high-affinity iron uptake in yeast. Science **271:**1552-1557.

35. **Urbanowski, J. L., and R. C. Piper.** 1999. The iron transporter Fth1p forms a complex with the Fet5 iron oxidase and resides on the vacuolar membrane. J. Biol. Chem. **274:**38061-38070.

36. **Volland, C., D. Urban-Grimal, G. Geraud, and R. Haguenauer-Tsapis.** 1994. Endocytosis and degradation of the yeast uracil permease under adverse conditions. J. Biol. Chem. **269:**9833-9841.

37. **Yamaguchi-Iwai, Y., A. Dancis, and R. D. Klausner.** 1995. *AFT1*: a mediator of iron regulated transcriptional control in *Saccharomyces cerevisiae*. EMBO J. **14:**1231-1239.

38. **Yamaguchi-Iwai, Y., R. Stearman, A. Dancis, and R. D. Klausner.** 1996. Iron-regulated DNA binding by the AFT1 protein controls the iron regulon in yeast. EMBO J. **15:**3377-3384.

39. **Yamaguchi-Iwai, Y., R. Ueta, A. Fukunaka, and R. Sasaki.** 2002. Subcellular localization of Aft1 transcription factor responds to iron status in Saccharomyces cerevisiae. J. Biol. Chem. **277:**18914-18918.

40. **Yuan, D. S., R. Stearman, A. Dancis, T. Dunn, T. Beeler, and R. D. Klausner.** 1995. The Menkes/Wilson disease gene homologue in yeast provides copper to a ceruloplasmin-like oxidase required for iron uptake. Proc. Natl. Acad. Sci. USA **92:**2632-2636.

41. **Yun, C. W., M. Bauler, R. E. Moore, P. E. Klebba, and C. C. Philpott.** 2001. The role of the FRE family of plasma membrane reductases in the uptake of siderophore-iron in Saccharomyces cerevisiae. J. Biol. Chem. **276:**10218-10223.

42. **Yun, C. W., T. Ferea, J. Rashford, O. Ardon, P. O. Brown, D. Botstein, J. Kaplan, and C. C. Philpott.** 2000. Desferrioxamine-mediated iron uptake in *Saccharomyces cerevisiae*. Evidence for two pathways of iron uptake. J. Biol. Chem. **275:**10709-10715.

43. **Yun, C. W., J. S. Tiedeman, R. E. Moore, and C. C. Philpott.** 2000. Siderophore-iron uptake in *Saccharomyces cerevisiae.* Identification of ferrichrome and fusarinine transporters. J. Biol. Chem. **275:**16354-16359.

44. **Zhao, H., and D. Eide.** 1996. The yeast *ZRT1* gene encodes the zinc transporter protein of a high-affinity uptake system induced by zinc limitation. Proc. Natl. Acad. Sci. USA **93:**2454-2458.

Table I. *Saccharomyces cerevisiae* strains used

Strain	Genotype	Reference
CM3260	*MATα trp1-63 leu2-3 112 gcn4-101 his3-309*	(37)
Y18	*MATα trp1-63 leu2-3 112 gcn4-101 his3-309 aft1 : :TRP1*	(37)
Y18 *aft2*Δ	*MATα trp1-63 leu2-3 112 gcn4-101 his3-309 aft1 : :TRP1 aft2 : :kanMX4*	(3)
BY4741	*MATa his3Δ1 leu2Δ0 met15Δ0 ura3Δ0*	Euroscarf
BY4742	*MATα his3Δ1 leu2Δ0 lys2Δ0 ura3Δ0*	Euroscarf
Y01090	*MATa his3Δ1 leu2Δ0 met15Δ0 ura3Δ0 aft2 : :kanMX4*	Euroscarf
Y14438	*MATα his3Δ1 leu2Δ0 lys2Δ0 ura3Δ0 aft1 : :kanMX4*	Euroscarf
Y11090	*MATα his3Δ1 leu2Δ0 lys2Δ0 ura3Δ0 aft2 : :kanMX4*	Euroscarf
SCMC01	*MATα his3Δ1 leu2Δ0 lys2Δ0 ura3Δ0 aft1 : :kanMX4 aft2 : :kanMX4*	This study
SCMC05	*MATα his3Δ1 leu2Δ0 lys2Δ0 ura3Δ0 AFT1-3HA : :HIS3MX6*	This study
SCMC11	*MATa his3Δ1 leu2Δ0 met15Δ0 ura3Δ0 AFT2-3HA : :HIS3MX6*	This study
SCMC18	*MATα his3Δ1 leu2Δ0 ura3Δ0 AFT2-3HA : :HIS3MX6*	This study
SCMC13	*MATα his3Δ1 leu2Δ0 ura3Δ0 aft1 : :kanMX4 AFT2-3HA : :HIS3MX6*	This study
SCMC10	*MATα his3Δ1 leu2Δ0 ura3Δ0 aft2 : :kanMX4 AFT1-3HA : :HIS3MX6*	This study

Table II. Primer sets for the PCR amplifications used in the ChIP assays and Northern Blots

	Chromatin Immunoprecipitation	
	Upper primer	**Lower primer**
Negative controls		
POL1	GCCGCTCGAAATGGTACATC	GCAATTCCTGGCGCTTTCT
RPO21	GTTCGTTGATCGTACCTTACCTCAT	GATAAGACCTTCACGACCACCC
Promoter gene		
FET3	AGTACGCTGAGTCGCCGATAA	CGAGAATAAGAGCACCTGCAAA
FTR1	GTGCGCGAATACTGCTGGT	TTACTGCTGCGACGGTGCT
MRS4	TAACCCACAGGAATCGCTACTTT	GGTGTTCTTGCCTTTCAGTCTTC
SMF3	ACATTGAAGCCACGACAAATGA	ACAGGGTGCGGTTACCATGA

	Northern Blot	
	Upper primer	**Lower primer**
Coding sequence		
FET3	TTCTTGGACGATTTCTACTT	GCAACTCTGGCAAACTTCTA
FTR1	TCCGTGCTGCTATCGTTTTT	ATCCCACCCATTGTCCAGTT
MRS4	ATGGAGCATTCTTTGATGTT	ATTAGCCACTATCCTTGGTT
SMF3	CTGAAAACTGTCGTCATAAT	AGGACAAGACCACTTGAGA

FIGURE LEGENDS

Figure 1- *Cluster analysis of DNA microarray hybridization with the wild type, aft1 and aft1aft2 strains grown in iron-depleted conditions.*

Each column displays the results from two experiments and cells represent the averaged ratio of mRNAs (strain1/strain2). Transcripts more abundant in strain 1 are in red, transcripts more abundant in strain 2 are in green. The scale indicates the magnitude of the expression ratio. The *AFT1-1^{up}* (1up) or the *AFT2-1^{up}* (2up) activation from previous studies (29, 30, 33) is indicated. Gene functions are described according to the *Saccharomyces cerevisiae* Genome Database. Genes selected for Northern blotting and ChIP analyses are indicated in bold. The number of MEME consensus sites within the 700 bp of the promoter of each gene is indicated.

Figure 2- *Probability-based motif derived from MEME analysis of genes in classes A-E*.

The letter-probability matrix of the motif is based on the elements within the 700 bp promoters of genes from each class. The scale indicates the probability of each possible base occurring at each position in the motif multiplied by 10 and rounded to the nearest integer. The most probable form of the motif (the MEME consensus) derived from the probability matrix is shown. The putative consensus binding sites for Aft1 and Aft2 in the DNA sequences upstream of the 50 genes up-regulated by *AFT1-1^{up}* and/or *AFT2-1^{up}* are shown. Boxed, dark gray nucleotides are identical to the consensus identified by MEME, and boxed, light gray nucleotides are found in more than 50 % of the analyzed sequences. Numbering corresponds to + 1 at the putative translation start site.

Figure 3- *Effects of Aft1 and Aft2 on FET3 regulation*.

(A and C) Northern blot analysis of *FET3* transcription. (A) Cells were grown exponentially in iron-depleted conditions (-Fe). (C) Cells were grown exponentially in iron-replete conditions (+Fe). Identical amounts of total RNA extracted from the indicated strains were blotted onto a

nylon membrane and hybridized with the indicated probes. The plasmids designated 2μ*AFT1* and 2μ*AFT2* are derivatives of plasmid pEG202 (see Materials and Methods). Experiments were repeated twice with similar results. Data from a single experiment are presented. Numbers represent the *FET3* signal after normalization with the *ACT1* signal. 100% refers to the transcription of *FET3* in the wild type strain under-iron depleted conditions. (B and D) *In vivo* DNA binding of Aft1-HA and Aft2-HA to the *FET3* promoter. Strains containing Aft1-HA in a wild type (*AFT2*, *AFT1-HA*) or *aft2*Δ context (*aft2*Δ, *AFT1-HA*) and strains containing Aft2-HA in a wild type (*AFT1*, *AFT2-HA*) or *aft1*Δ context (*aft1*Δ, *AFT2-HA*) were grown exponentially in iron-depleted conditions (B). Strains showing significant specific binding of Aft1-HA or Aft2-HA to the *FET3* promoter were also grown in iron-replete conditions (D). ChIP experiments were performed as described in Materials and Methods. Samples (immunoprecipitated DNA, beads alone control DNA, and total DNA) were amplified with the specified primer pairs. The height of the bars represents the specific protein occupancy calculated as described in Materials and Methods. Error bars represent the standard deviation resulting from 2 independent experiments. The fold enrichment is defined as the protein occupancy of the *FET3* promoter normalized to the average protein occupancy of the negative controls *POL1* and *RPO21*.

Figure 4- *Effects of Aft1 and Aft2 on FTR1 regulation.*

(A and C) Northern blot analysis of *FTR1* transcription. Cells grown exponentially in iron-depleted (A) or iron-replete conditions (C) were analyzed as in figure 3. 100% is the transcription of *FET3* in the wild type strain under iron-depleted conditions. (B and D) *In vivo* DNA binding of Aft1-HA and Aft2-HA to the *FTR1* promoter. Strains containing Aft1-HA in a wild type (*AFT2*, *AFT1-HA*) or *aft2*Δ context (*aft2*Δ, *AFT1-HA*) and strains containing Aft2-HA in a wild type (*AFT1*, *AFT2-HA*) or *aft1*Δ context (*aft1*Δ, *AFT2-HA*) were grown exponentially in iron-depleted conditions (B). Strains showing significant specific binding of

Aft1-HA or Aft2-HA to the *FTR1* promoter were also grown in iron-replete conditions (D). ChIP experiments and analyses were performed as described in Materials and Methods and figure 3.

Figure 5- *Effects of Aft1 and Aft2 on SMF3 regulation.*

(A and C) Northern blot analysis of *SMF3* transcription. Strains were grown in iron-depleted (A) or iron-replete (C) medium and analyzed as in figure 3. 100% is the transcription of *FET3* in the wild type strain under iron-depleted conditions. (B and D) *In vivo* DNA-binding of Aft1 and Aft2 to the *SMF3* promoter. Strains containing Aft1-HA in a wild type (*AFT2*, *AFT1-HA*) or *aft2*Δ context (*aft2*Δ, *AFT1-HA*) and strains containing Aft2-HA in a wild type (*AFT1*, *AFT2-HA*) or *aft1*Δ context (*aft1*Δ, *AFT2-HA*) were grown exponentially in iron-depleted conditions (B). Strains showing significant specific binding of Aft1-HA or Aft2-HA to the *SMF3* promoter were also grown in iron-replete conditions (D). ChIP experiments and analyses were performed as described in Materials and Methods and figure 3.

Figure 6- *Effects of Aft1 and Aft2 on MRS4 regulation.*

(A and C) Northern blot analysis of *MRS4* transcription. Cells were grown exponentially in iron-depleted (A) or iron-replete conditions (C) and analyzed as described in figure 3. 100% is the transcription of *FET3* in the wild type strain under iron-depleted conditions.(B and D) *In vivo* DNA-binding of Aft1 and Aft2 to the *MRS4* promoter. Strains containing Aft1-HA in a wild type (*AFT2*, *AFT1-HA*) or *aft2*Δ context (*aft2*Δ, *AFT1-HA*) and strains containing Aft2-HA in a wild type (*AFT1*, *AFT2-HA*) or *aft1*Δ context (*aft1*Δ, *AFT2-HA*) were grown exponentially in iron-depleted conditions (B). Only the strain containing Aft2-HA in an *aft1*Δ context (*aft1*Δ, *AFT2-HA*) was grown in iron-replete conditions (D). ChIP experiments and analyses were performed as described in Materials and Methods and figure 3.

Figure 7- *Mutational analysis of the FET3 regulatory sequence.*

(A) Plasmid pFC-W contains the -263/-234 of the upstream region of the *FET3* gene that has been inserted into the *CYC1* promoter and fused to the *LacZ* gene (38). Plasmid pFC-M1 is identical to the pFC-W, except that the di-nucleotide GT flanking the 5' *FET3* core sequence GCACCC was replaced by the di-nucleotide CC that flanks the 5' *SMF3* GCACCC sequence (Fig.2). Plasmid pFC-M2 is identical to the pFC-W, except that the di-nucleotide AT flanking the 3' *FET3* GCACCC sequence was replaced by the di-nucleotide TG, flanking the 3' *SMF3* GCACCC sequence. Plasmid pFC-M3 contains both substitutions (GT to CC and AT to TG) of the pFC-M1 and pFC-M2 plasmids. The 5' *FET3* core sequence GCACCC is represented in bold. Nucleotides that deviate from the *FET3* sequence are underlined. (B) The strains BY4742 (WT), Y14438 (*aft1Δ*), Y11090 (*aft2Δ*), SCMC01 (*aft1Δaft2Δ*), harbouring the plasmids pFC-W, pFC-M1, pFC-M2 or pFC-M3, with or without overexpression of *AFT1* or *AFT2* (plasmids pEG202-*AFT1* and pEG202-*AFT2*, see Materials and Methods) were grown for 18h in iron-limiting medium containing 1μM iron, then diluted to an $OD_{600\ nm}$ = 0.3 in the same medium without iron and grown to an $OD_{600\ nm}$ = 1.0. Error bars represent the standard deviation (less than 10%) for assays performed on three independent transformants. Numerical values of β-galactosidase activities are shown in the lower panel.

Figure 8- *Analysis of the relative abundances of Aft1 and Aft2*.

Equal amounts of total protein extract from cells grown exponentially in iron-depleted (-Fe) or iron-replete medium (+Fe) were analyzed by western blotting with an anti-HA antibody to detect HA-tagged Aft1 in wild type and *aft2*Δ strains (A), and HA-tagged Aft2 in wild type and *aft1*Δ strains (B). Aft1 and Aft2 were assayed after the same exposure times. Results from two independent protein extracts are shown in bar graphs after normalization to the Pgk1 signal. The amounts of Aft1 and Aft2 in the wild type context in iron-deplete conditions were arbitrarily defined as 100%.

Figure 9- *Diagram of Aft1 and Aft2 DNA binding activities and protein amounts in iron-depleted conditions.*

*(A) The bars represent the promoter occupancy by Aft1 in the aft2*Δ strain (black bars) and promoter occupancy by Aft2 in the *aft1*Δ strain (white bars). The heights of the bars is proportional to each calculated fold enrichment from figure 3 (*FET3*), figure 4 (*FTR1*), figure 5 (*SMF3*) and figure 6 (*MRS4*). (B) The amounts of Aft1 and Aft2 proteins are represented by spheres with areas proportional to the protein measured in figure 7. Aft1 is in black, and Aft2 is in white.

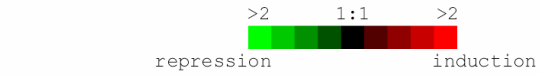

1: wt/*aft1*
2: wt/*aft1aft2*
3: *aft1*/*aft1aft2*

	1 2 3	Gene name	up regulation	Function	Number of MEME consensus
A		*ARN1*	1up	Iron-siderochrome transporter	1 (-260)
		AHP1	2up	Thioredoxine peroxidase, cell redox homeostasis	0
		FRE1	1up/2up	Metalloreductase, iron/copper transport	0
		ARN4	1up	Iron-siderochrome transporter	2 (-137/-193)
		ZPS1	2up	Putative GPI-anchored protein	0
		FET3	1up/2up	Multicopper oxidase, ferrous iron transport	1 (-251)
		FIT2	1up/2up	Cell wall protein, iron transport	4 (-131/-249/-266/-331)
		YOR387C	1up		0
		FIT3	1up/2up	Cell wall protein, iron transport	1 (-184)
		ARN2	1up	Iron-siderochrome transporter	1 (-447)
		BIO5	1up	Biotin transport	0
		PRB1	2up	Vacuolar proteinase B	2 (-378/-504)
		ARN3	1up	Iron-siderochrome transporter	1 (-188)
B		*FRE2*	1up	Metalloreductase, iron transport	1 (-430)
		CCC2	1up	Copper-transporting P-type ATPase, iron transport	2 (-242/-290)
		CTH2	1up/2up	Zinc finger containing homolog of mammalian *TIS11*	2 (-173/-249)
		ZRT1	2up	High-affinity zinc transporter	0
		FTR1	1up/2up	High affinity iron permease, ferrous iron transport	2 (-175/-365)
		HMX1	1up	Heme oxygenase, iron homeostasis	1 (-451)
C		*ECM4*	2up		1 (-147)
		COT1	1up/2up	Vacuolar cobalt/zinc transporter	1 (-285)
		HSP26	2up	Unfolded protein binding, response to stress	1 (-302)
		LAP4	2up	Vacuolar aminopeptidase I	1 (-137)
		AKR1	1up	Palmitoyltransferase, endocytosis	1 (-163)
		YDL124W	2up		0
		FRE6	1up	Metalloreductase	2 (-141/-168)
		FTH1	1up/2up	Similar to *FTR1*, vacuolar iron transport	1 (-177)
		SMF3	1up/2up	Vacuolar iron transporter	2 (-360/-429)
		PEP4	2up	Vacuolar proteinase A	1 (-368)
D		*CAD1*	2up	Transcriptional activator, response to cadmium	1 (-52)
		MRS4	2up	Mitochondrial carrier protein, iron transport	3 (-192/-237/-270)
		FET5	2up	Similar to *FET3*, vacuolar iron transport	2 (-127/-620)
		BNA2	2up	Tryptophan 2,3-dioxygenase, NAD biosynthesis	1 (-342)
		YOL083W	2up		1 (-190)
		FIT1	1up/2up	Cell wall protein, iron transport	3 (-181/-271/-283)
		VHT1	1up	Vitamin H transporter, biotin transport	1 (-69)
		HCR1	2up	Processing of 20S-rRNA and protein biosynthesis	0
		NFT1	2up	ATPase, transport	2 (-188/-324)
		YMR041C	2up		1 (-217)
		ISU1	2up	Iron-sulfur cluster protein, iron homeostasis	1 (-251)
		YGR146C	2up		2 (-354/-677)
E		*ATX1*	1up	Copper chaperone, iron transport	0
		FRE3	1up	Metalloreductase, iron transport	1 (-618)
		FRE5	1up	Metalloreductase	2 (-229/-330)
		GRX4	2up	Glutaredoxine, response to oxidative stress	0
		YHL035C	1up/2up	Member of the ATP-binding cassette family	0
		FRE4	1up	Metalloreductase, iron transport	1 (-436)
		UBC8	1up	Ubiquitin-conjugating enzyme	0
		OYE3	1up/2up	NADPH oxidoreductase	0
		YMR034C	1up	Sterol transporter	1 (-86)

Figure 1

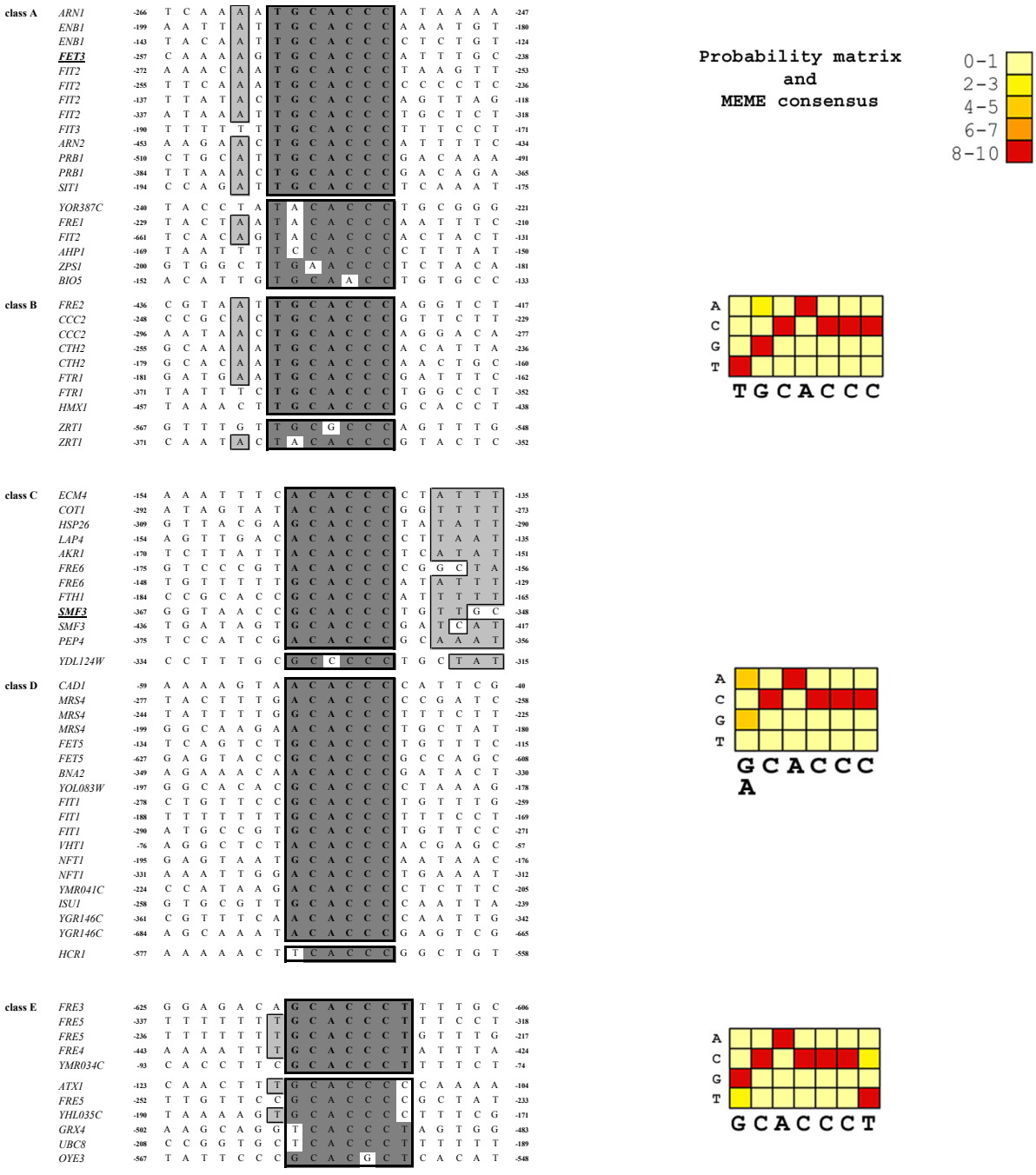
class A
ARN1 -266 T C A A A A T G C A C C C A T A A A A -247
ENB1 -199 A A T T A T T G C A C C C A A A T G T -180
ENB1 -143 T A C A A T T G C A C C C C T C T G T -124
FET3 -257 C A A A A G T G C A C C C A T T T G C -238
FIT2 -272 A A A C A A T G C A C C C T A A G T T -253
FIT2 -255 T T C A A A T G C A C C C C C C T C -236
FIT2 -137 T T A T A C T G C A C C C A G T T A G -118
FIT2 -337 A T A A A A T T G C A C C C T G C T C T -318
FIT3 -190 T T T T T T T G C A C C C T T T C C T -171
ARN2 -453 A A G A A C T G C A C C C A T T T T C -434
PRB1 -510 C T G C A T T G C A C C C G A C A A A -491
PRB1 -384 T T A A A C T G C A C C C G A C A G A -365
SIT1 -194 C C A G A T T G C A C C C T C A A A T -175
YOR387C -240 T A C C T A T A C A C C C T G C G G G -221
FRE1 -229 T A C T A A T A C A C C C A A T T T C -210
FIT2 -661 T C A C A G T A C A C C C A C T A C T -131
AHP1 -169 T A A T T T T C C A C C C C T T T A T -150
ZPS1 -200 G T G G C T T G A C C C T C T A C A -181
BIO5 -152 A C A T T G T G C A A C C T G T G C C -133
class B
FRE2 -436 C G T A A T T G C A C C C A G G T C T -417
CCC2 -248 C C G C A C T G C A C C C G T T C T T -229
CCC2 -296 A A T A A C T G C A C C C A G G A C A -277
CTH2 -255 G C A A A A T G C A C C C A C A T T A -236
CTH2 -179 G C A C A A T G C A C C C A A C T G C -160
FTR1 -181 G A T G A A T G C A C C C G A T T T C -162
FTR1 -371 T A T T T C T G C A C C C T G G C C T -352
HMX1 -457 T A A A C T T G C A C C C G C A C C T -438
ZRT1 -567 G T T T G T T G C G C C C A G T T T G -548
ZRT1 -371 C A A T A C T A C A C C C G T A C T C -352
class C
ECM4 -154 A A A T T T C A C A C C C C T A T T T -135
COT1 -292 A T A G T A T A C A C C C G G T T T T -273
HSP26 -309 G T T A C G A G C A C C C T A T A T T -290
LAP4 -154 A G T T G A C A C A C C C C T T A A T -135
AKR1 -170 T C T T A T T A C A C C C T C A T A T -151
FRE6 -175 G T C C C G T A C A C C C C G G C T A -156
FRE6 -148 T G T T T T T G C A C C C A T A T T T -129
FTH1 -184 C C G C A C C G C A C C C A T T T T T -165
SMF3 -367 G G T A A C C G C A C C C T G T T G C -348
SMF3 -436 T G A T A G T G C A C C C G A T C A T -417
PEP4 -375 T C C A T C G A C A C C C G C A A A T -356
YDL124W -334 C C T T T G C G C C C C T G C T A T -315
class D
CAD1 -59 A A A A G T A A C A C C C C A T T C G -40
MRS4 -277 T A C T T T G A C A C C C C C G A T C -258
MRS4 -244 T A T T T T G G C A C C C T T T C T T -225
MRS4 -199 G G C A A G A A C A C C C T G C T A T -180
FET5 -134 T C A G T C T G C A C C C T G T T T C -115
FET5 -627 G A G T A C C G C A C C C G C C A G C -608
BNA2 -349 A G A A A C A A C A C C C G A T A C T -330
YOL083W -197 G G C A C A C G C A C C C C T A A A G -178
FIT1 -278 C T G T T C C G C A C C C T G T T T G -259
FIT1 -188 T T T T T T T G C A C C C T T T C C T -169
FIT1 -290 A T G C C G T G C A C C C T G T T C C -271
VHT1 -76 A G G C T C T A C A C C C A C G A G C -57
NFT1 -195 G A G T A A T G C A C C C A A T A A C -176
NFT1 -331 A A A T T G G A C A C C C T G A A A T -312
YMR041C -224 C C A T A A G A C A C C C C T C T T C -205
ISU1 -258 G T G C G T T G C A C C C C A A T T A -239
YGR146C -361 C G T T T C A A C A C C C C A A T T G -342
YGR146C -684 A G C A A A T A C A C C C G A G T C G -665
HCR1 -577 A A A A A C T T C A C C C G G C T G T -558
class E
FRE3 -625 G G A G A C A G C A C C C T T T T G C -606
FRE5 -337 T T T T T T T T G C A C C C T T T C C T -318
FRE5 -236 T T T T T T T T G C A C C C T G T T T G -217
FRE4 -443 A A A A T T T T G C A C C C T A T T T A -424
YMR034C -93 C A C C T T C G C A C C C T T T T C T -74
ATX1 -123 C A A C T T T G C A C C C C C A A A A -104
FRE5 -252 T T G T T C C C G C A C C C C G C T A T -233
YHL035C -190 T A A A A G T G C A C C C C T T T C G -171
GRX4 -502 A A G C A G G T C A C C C T A G T G G -483
UBC8 -208 C C G G T G C T C A C C C T T T T T T -189
OYE3 -567 T A T T C C C G C A C G C T C A C A T -548
Probability matrix
and
MEME consensus
0-1
2-3
4-5
6-7
8-10
A
C
G
T
TGCACCC
A
C
G
T
GCACCC
A
A
C
G
T
GCACCCT

Figure 2

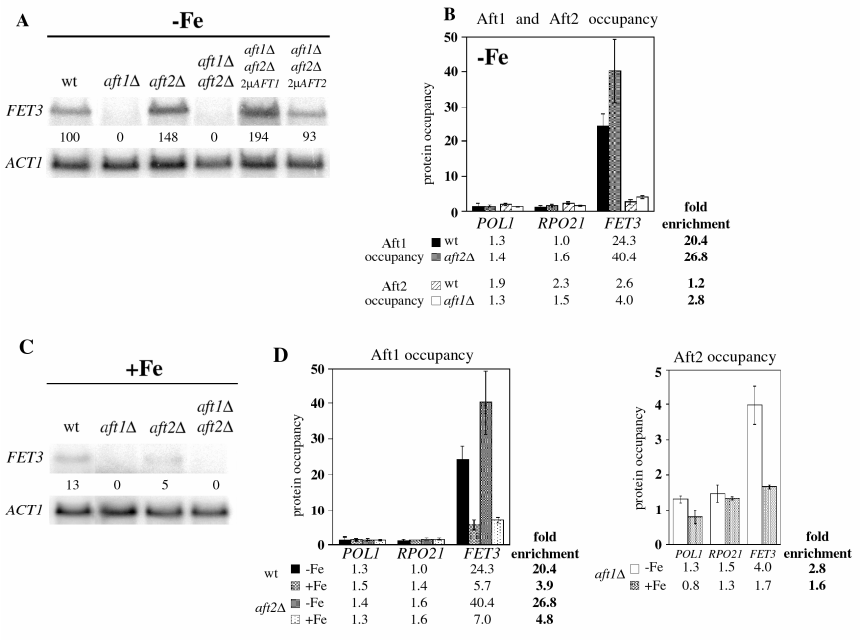
A
-Fe
wt
aft1Δ
aft2Δ
aft1Δ aft2Δ
aft1Δ aft2Δ 2μAFT1
aft1Δ aft2Δ 2μAFT2
FET3
100 0 148 0 194 93
ACT1
B
Aft1 and Aft2 occupancy
-Fe
protein occupancy
POL1 RPO21 FET3 fold enrichment
Aft1 occupancy wt 1.3 1.0 24.3 20.4
aft2Δ 1.4 1.6 40.4 26.8
Aft2 occupancy wt 1.9 2.3 2.6 1.2
aft1Δ 1.3 1.5 4.0 2.8
C
+Fe
wt
aft1Δ
aft2Δ
aft1Δ aft2Δ
FET3
13 0 5 0
ACT1
D
Aft1 occupancy
protein occupancy
POL1 RPO21 FET3 fold enrichment
wt -Fe 1.3 1.0 24.3 20.4
+Fe 1.5 1.4 5.7 3.9
aft2Δ -Fe 1.4 1.6 40.4 26.8
+Fe 1.3 1.6 7.0 4.8
Aft2 occupancy
protein occupancy
POL1 RPO21 FET3 fold enrichment
aft1Δ -Fe 1.3 1.5 4.0 2.8
+Fe 0.8 1.3 1.7 1.6

Figure 3

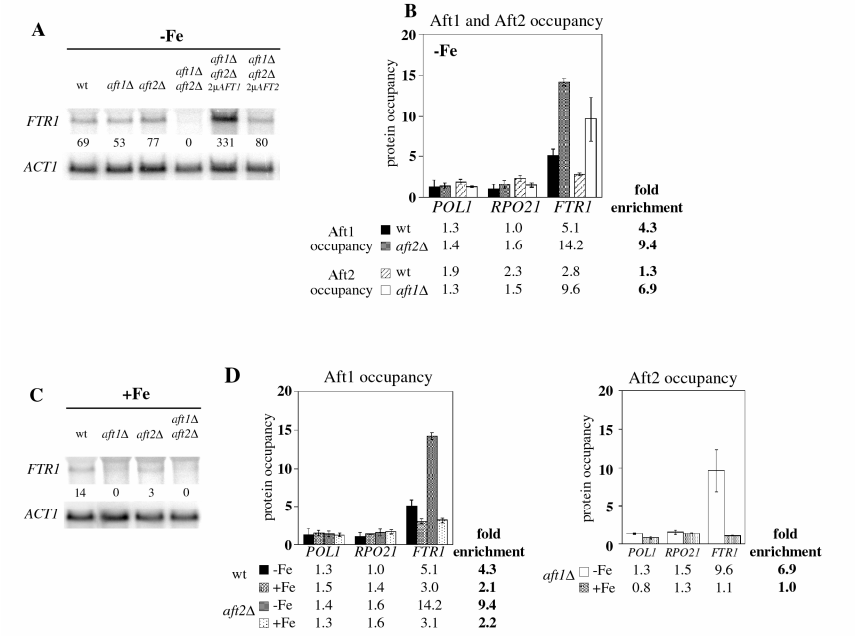
A
-Fe
wt
aft1Δ
aft2Δ
aft1Δ aft2Δ 2μAFT1
aft1Δ aft2Δ 2μAFT2
FTR1
69
53
77
0
331
80
ACT1
B
Aft1 and Aft2 occupancy
-Fe
protein occupancy
POL1
RPO21
FTR1
fold enrichment
Aft1 occupancy
wt 1.3 1.0 5.1 4.3
aft2Δ 1.4 1.6 14.2 9.4
Aft2 occupancy
wt 1.9 2.3 2.8 1.3
aft1Δ 1.3 1.5 9.6 6.9
C
+Fe
wt
aft1Δ
aft2Δ
aft1Δ aft2Δ
FTR1
14
0
3
0
ACT1
D
Aft1 occupancy
wt -Fe 1.3 1.0 5.1 4.3
+Fe 1.5 1.4 3.0 2.1
aft2Δ -Fe 1.4 1.6 14.2 9.4
+Fe 1.3 1.6 3.1 2.2
Aft2 occupancy
aft1Δ -Fe 1.3 1.5 9.6 6.9
+Fe 0.8 1.3 1.1 1.0

Figure 4

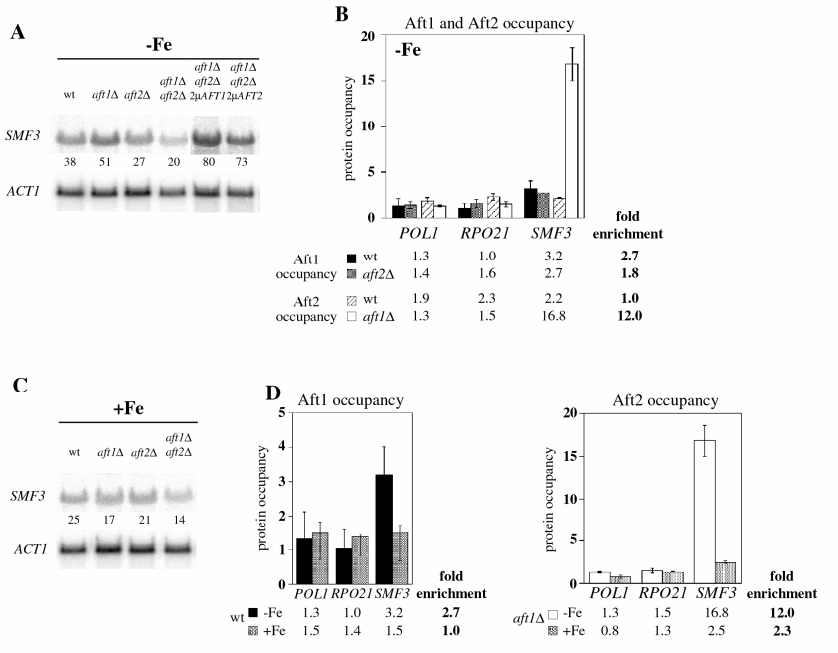
A
-Fe
wt
aft1Δ
aft2Δ
aft1Δ aft2Δ
aft1Δ aft2Δ 2μAFT1
aft1Δ aft2Δ 2μAFT2
SMF3
38 51 27 20 80 73
ACT1
B
Aft1 and Aft2 occupancy
-Fe
protein occupancy
POL1 RPO21 SMF3
fold enrichment
Aft1 occupancy wt 1.3 1.0 3.2 2.7
aft2Δ 1.4 1.6 2.7 1.8
Aft2 occupancy wt 1.9 2.3 2.2 1.0
aft1Δ 1.3 1.5 16.8 12.0
C
+Fe
wt
aft1Δ
aft2Δ
aft1Δ aft2Δ
SMF3
25 17 21 14
ACT1
D
Aft1 occupancy
protein occupancy
POL1 RPO21 SMF3
fold enrichment
wt -Fe 1.3 1.0 3.2 2.7
+Fe 1.5 1.4 1.5 1.0
Aft2 occupancy
protein occupancy
POL1 RPO21 SMF3
fold enrichment
aft1Δ -Fe 1.3 1.5 16.8 12.0
+Fe 0.8 1.3 2.5 2.3

Figure 5

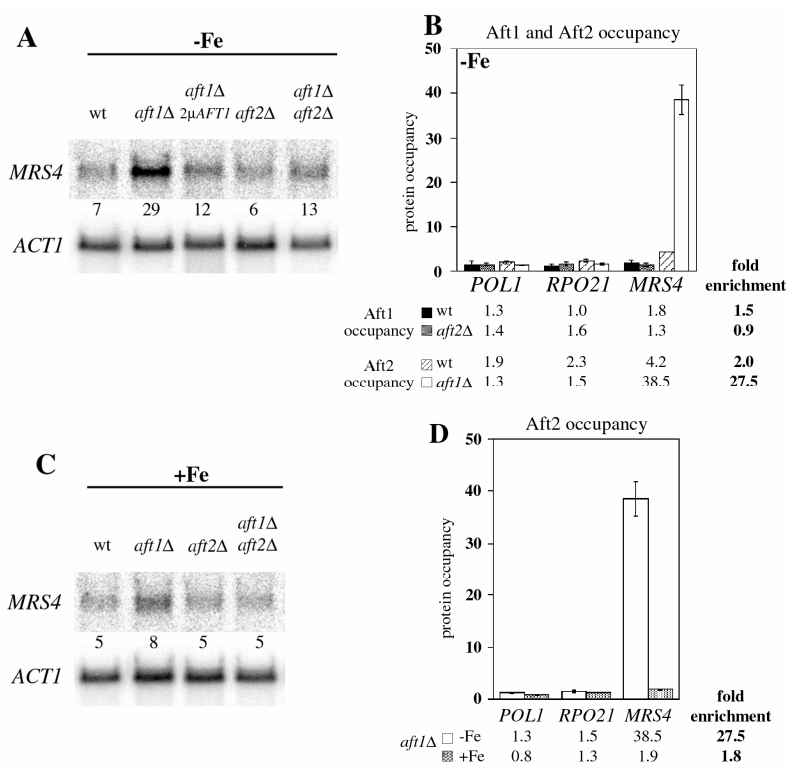
A
-Fe
wt
aft1Δ
aft1Δ 2μAFT1
aft2Δ
aft1Δ aft2Δ
MRS4
7
29
12
6
13
ACT1
B
Aft1 and Aft2 occupancy
-Fe
protein occupancy
POL1
RPO21
MRS4
fold enrichment
Aft1 occupancy ■ wt 1.3 1.0 1.8 1.5
■ aft2Δ 1.4 1.6 1.3 0.9
Aft2 occupancy ▨ wt 1.9 2.3 4.2 2.0
□ aft1Δ 1.3 1.5 38.5 27.5
C
+Fe
wt
aft1Δ
aft2Δ
aft1Δ aft2Δ
MRS4
5
8
5
5
ACT1
D
Aft2 occupancy
protein occupancy
POL1
RPO21
MRS4
fold enrichment
aft1Δ □ -Fe 1.3 1.5 38.5 27.5
▨ +Fe 0.8 1.3 1.9 1.8

Figure 6

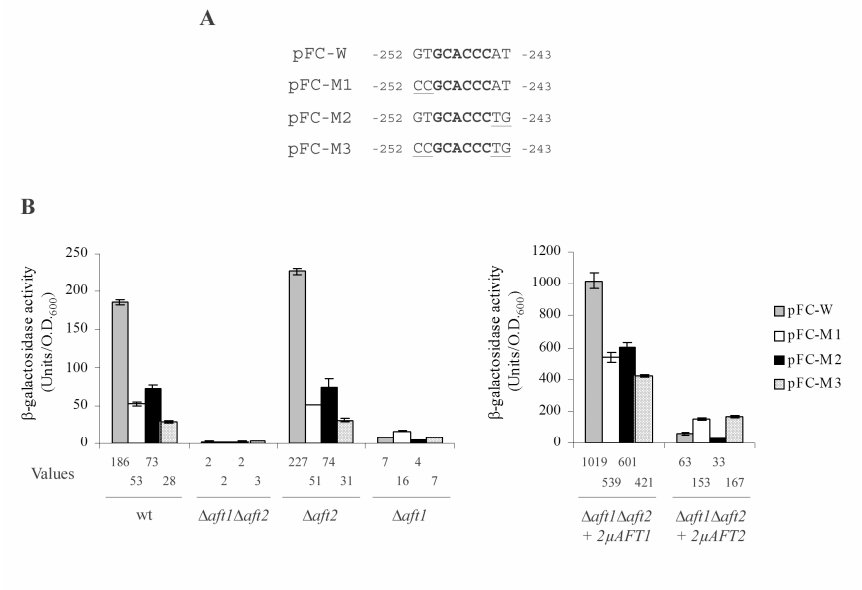
A
pFC-W -252 GTGCACCCAT -243
pFC-M1 -252 CCGCACCCAT -243
pFC-M2 -252 GTGCACCCTG -243
pFC-M3 -252 CCGCACCCTG -243
B
β-galactosidase activity (Units/O.D600)
250
200
150
100
50
0
Values
186 73
53 28
2 2
2 3
227 74
51 31
7 4
16 7
wt
Δaft1Δaft2
Δaft2
Δaft1
1200
1000
800
600
400
200
0
1019 601
539 421
63 33
153 167
Δaft1Δaft2 + 2μAFT1
Δaft1Δaft2 + 2μAFT2
pFC-W
pFC-M1
pFC-M2
pFC-M3

Figure 7

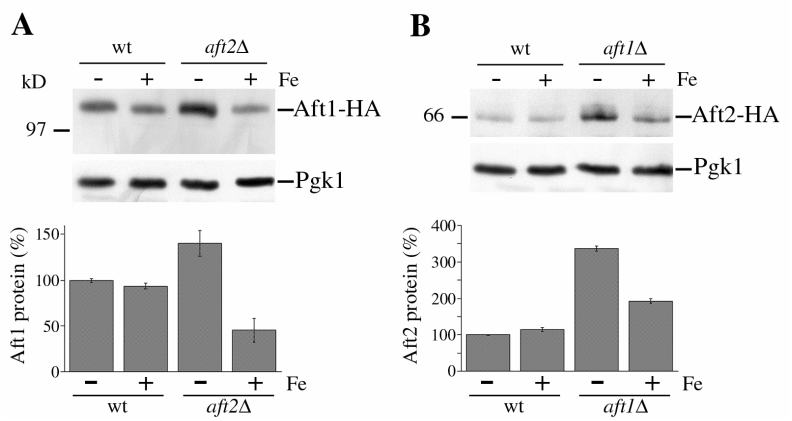
A
wt
aft2Δ
kD
-
+
-
+
Fe
97
Aft1-HA
Pgk1
Aft1 protein (%)
150
100
50
0
B
wt
aft1Δ
66
Aft2-HA
Pgk1
Aft2 protein (%)
400
300
200
100
0

Figure 8

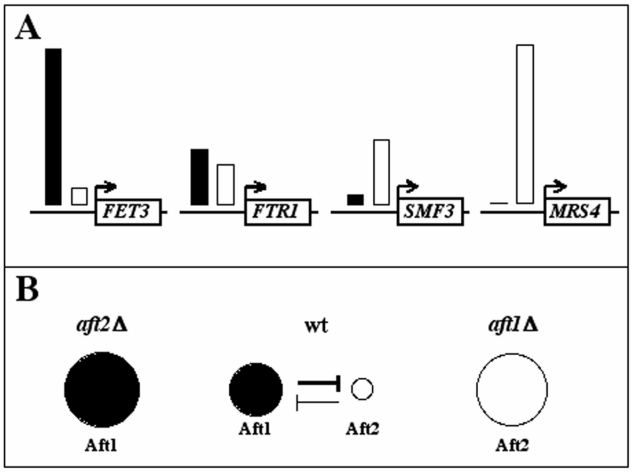

Figure 9